from −7 to 0V, step of 0.2V and drain voltage from 0 to 30V, step of 3V. We can see that Gm of proposed device (blank color square) is larger and flatter than compared device (red color circle). It denotes that proposed device has better linearity than compared device. Figure 5 shows that power gain, output power (Pout) and power added efficiency (PAE) of both devices change with input power (Pin). When input power is less than 3 dBm, gain and output power of both devices are almost the same, and when input power is more than 3 dBm, gain and output power of proposed device (black color square) is larger than ones of compared device (red color circle). When input power is less than 9 dBm, PAE of proposed device (black color square) is less than one of compared device (red color circle), and when input power is more than 9 dBm, PAE of proposed device (black color square) is larger than one of compared device (red color circle).

5. CONCLUSIONS

This article proposes a novel $Al_{0.27}Ga_{0.73}N$ /AlN/$Al_{0.04}Ga_{0.96}N$/GaN HEMT with composited -layer and unintentionally doping barrier based on theory calculation and TCAD software analysis. By fabrication, measured results show that proposed $Al_{0.27}Ga_{0.73}N$/AlN/$Al_{0.04}Ga_{0.96}N$/GaN HEMT with composited-layer has higher linearity and drain current density than compared device without composited-layer. Its gain, output power and PAE are improved a little too. It demonstrates propose device is benefit to design linear power amplifier applied to wireless communication system.

ACKNOWLEDGMENTS

The authors thank the support of National Natural Science Foundation of China (Grant No 60776052). Material and process of devices were provided by Science and Technology on ASIC Laboratory, Hebei Semiconductor Research Institute.

REFERENCES

1. Y.S. Lee, M.W. Lee, and Y.H. Jeong, A highly linear and efficient two-stage GaN HEMT asymmetrical Doherty amplifier for WCDMA application, Microwave Opt Technol Lett 51 (2008), 1464–1467.
2. P. Saad, C. Fager, H. Cao, H. Zirath, and K. Andersson, Design of a highly efficient 2–4-GHz octave bandwidth GaN-HEMT power amplifier, IEEE Trans Microwave Theory Tech 58 (2010), 1677–1685.
3. W. Saito, T. Nitta, Y. Kakiuchi, Y. Saito, K. Tsuda, I. Omura, and M. Yamaguchi, A 120-W boost converter operation using a high-voltage GaN-HEMT, IEEE Electron Device Lett 29 (2008), 8–10.
4. A.M. Darwidh, A.J. Bayba, and H.A. Hung, Thermal resistance calculation of AlGaN-GaN devices IEEE Trans Microwave Theory Tech 52 (2004), 2611–2620.
5. Z.Q. Cheng, J. Liu, Y.G. Zhou, K.J. Chen, and K.M. Lau, Broadband microwave noise characteristics of high-linearity composite-channel Al0.3Ga0.7N/Al0.05Ga0.95N/GaN HEMTs, IEEE Electron Device Lett 26 (2005), 521–523.
6. Z.Q. Cheng, Y. Cai, J. Liu, G.Y. Zhou, K.J. Chen, and K.M. Lau, 1.9GHz low noise amplifier using high linearity and low-noise composite-channel HEMTs, Microwave Opt Technol Lett 14 (2007), 1360–1362.
7. Z.Q. Cheng, Y. Cai, J. Liu, K.J. Chen, and K.M. Lau, A low phase-noise X-band MMIC VCO using high-linearity and low-noise composite-channel Al0.3Ga0.7N/Al0.05Ga0.95N/GaN HEMTs, IEEE Trans Microwave Theory Tech 55 (2007), 23–29.
8. S. Imanaga and H. Kawau, Novel AlN/GaN isulated gate heterostructure field effect transistor with modulation doping and one-dimensional simulation of charge control, J Appl Phys 82 (1997), 5843–5858.
9. C. Ostermaier, G. Pozzovivo, J.F. Carlin, B. Basnar, W. Schrenk, Y. Douvry, et al. Ultrathin InAlN/AlN barrier HEMT with high performance in normally off operation, IEEE Electron Device Lett 30 (2009), 1030–1032.
10. X.P Zhou, Z.Q. Cheng, S. Hu, W.J. Zhou, and S. Zhang, AlGaN/GaN HEMT device structure optimization design, IEEE Proceedings of International Symposium on the Physical and Failure Analysis of Integrated Circuits, Suzhou, China, 2009, pp. 339–343.
11. Z.Q. Cheng, X.P Zhou, S. Hu, W.J. Zhou, and S. Zhang, Optimization design of high linearity AlxGa1-xN/AlyGa1-yN/GaN high electron mobility transistor, Acta Phys Sin 59 (2010), 1252–1257.

CHANNEL CAPACITY STUDY OF POLARIZATION RECONFIGURABLE SLOT ANTENNA FOR INDOOR MIMO SYSTEM

Yue Li, Zhijun Zhang, Jianfeng Zheng, and Zhenghe Feng
State Key Lab of Microwave and Communications, Department of Electronic Engineering, Tsinghua University, Beijing, 100084, China; Corresponding author: zjzh@tsinghua.edu.cn

Received 24 August 2010

ABSTRACT: *This article presents a polarization reconfigurable slot antenna with compact feed. Fed by dual modes of coplanar waveguide, a dual orthogonal linear polarization is excited in the slot and controlled by two PIN diodes. The proposed antenna has been built and its reflection coefficient, radiation pattern, gain were tested. The capacity performance in an indoor wireless local area network scenario was measured by using two proposed antennas as access point in a 2 × 2 multi-input multi-output system. The results show the advantage of polarization reconfigurable antennas in channel capacity, especially at the condition of non-line-of-sight.* © 2011 Wiley Periodicals, Inc. Microwave Opt Technol Lett 53:1209–1213, 2011; View this article online at wileyonlinelibrary.com. DOI 10.1002/mop.26014

Key words: *polarization reconfigurable antenna; compact feed; channel capacity*

1. INTRODUCTION

Polarization reconfigurable antennas are widely studied and adopted in multi-input multi-output (MIMO) systems for their intrinsic polarization diversity advantage in mitigating the multipath fading and increasing the channel capacity, especially in polarization-varied environments [1–3]. The polarization property of such antennas can be switched between linear polarization (LP), left-hand circular polarization (LHCP), and right-hand circular polarization (RHCP), depending on the propagation environment. To achieve reconfigurable polarizations, several designs have been proposed in recent articles [4–6]. For example, two PIN diodes are implemented to control the reconfigurable polarization between LHCP and RHCP in a square slot antenna with wide bandwidth [4]. As studied in Ref. 5, a polarization switchable patch antenna is proposed, and its polarization modes are controlled by two PIN diodes among LHCP, RHCP, and two orthogonal LPs. As mentioned in Ref. 6, a polarization reconfigurable microstrip antenna with a piezoelectric transducer (PET) was designed and built. By controlling the bias voltage of the PET, it is possible to switch between LHCP and RHCP.

In this article, we will study the performance of polarization reconfigurable antennas in indoor MIMO system for wireless local area networks (WLAN) application. According to Ref. 4, the slot antenna has wider bandwidth with bidirectional

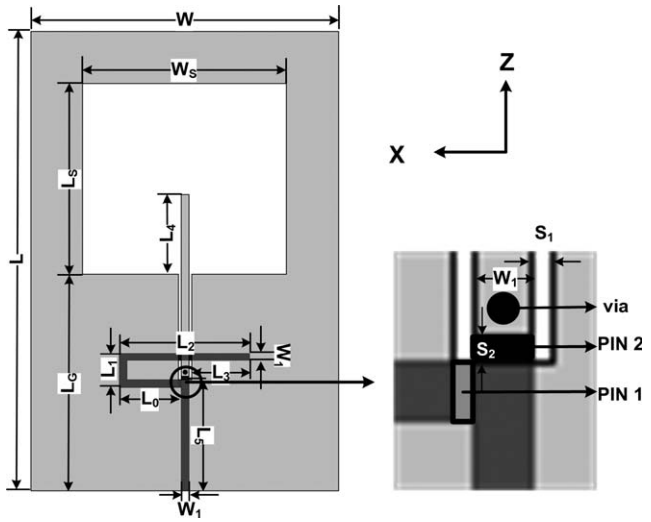

Figure 1 Geometry of proposed antenna

radiation, which meets the specification of an access point (AP). Therefore, a polarization reconfigurable slot antenna with compact feed is proposed as the antenna element in MIMO systems. Dual orthogonal linear polarizations are selected as diversity for better channel capacity. A prototype reconfigurable slot antenna is fabricated and measured, including the reflection coefficient, radiation pattern, and gain. To study its performance in indoor MIMO systems, two slot antennas serve as AP of a 2 × 2 WLAN MIMO system in a typical indoor scenario, in comparison with two dipoles with single polarization. The measured results illustrate that the channel capacity can be improved in both line-of-sight (LOS) and non-line-of-sight (NLOS) conditions.

2. ANTENNA DESIGN

The geometry of the proposed reconfigurable slot antenna element is shown in Figure 1. The antenna is composed of a rectangular slot, a coplanar waveguide (CPW), a capacitively coupled strip, and two PIN diodes. The rectangular slot with the dimensions of 53 × 50 mm^2 serves as the radiation aperture, etched in the front side of FR4 ($\varepsilon_r = 4.4$, $\tan\delta = 0.01$). A switchable feed, including a C-shaped capacitively coupled strip at the back side and a CPW at the front side through a via is controlled by two PIN diodes. To achieve different configuration of two PIN diodes, two orthogonal polarizations can be excited by two modes of the same CPW, which is shown in Table 1. Preliminary work about dual polarizations in slot is presented in Ref. 7. When PIN1 is ON and PIN2 is OFF, the antenna is fed through the C-shaped strip, which is capacitively coupled to the CPW. As a result, the horizontal polarization of the slot is excited. When PIN1 is OFF and PIN2 is ON, the vertical polarization is excited by typical CPW feed structure. Dual orthogonal polarizations are achieved by dual orthogonal modes of CPW independently, making the feed structure much more compact than the reference. Preliminary studies of parameter optimization are also discussed in Ref. 7, and the detailed values of each parameter are listed in Table 2.

TABLE 1 Working Configurations of PIN1 and PIN2

Mode	PIN1	PIN2	Polarization
1	ON	OFF	Horizontal
2	OFF	ON	Vertical

3. FABRICATION AND MEASUREMENTS

A prototype of the proposed reconfigurable slot antenna was fabricated and measured. The view of the front and back sides of the proposed antenna are shown in Figures 2(a) and 2(b), and the detailed bias circuits of two PIN diodes (D_1 and D_2, Philips BAP64-03) are shown in Figure 2(c). The ''ON'' and ''OFF'' states of the two PIN diodes are controlled by a single-pole 2-throw (SP2T) switch in the front side. The bias circuit consists of three RF choke inductances (L_{b1}, L_{b2}, and L_{b3}, 12 nH), a DC block capacitance (C_b, 120 pF), three RF-shorted capacitances (C_{s1}, C_{s2}, and C_{s3}, 470 pF), and a bias resistance (R, 46Ω).

The measured reflection coefficients for both polarizations are shown in Figure 3. They all agree well with the simulation. The −10-dB bandwidths are 700 MHz (2.02–2.72 GHz, 29.2%) and 940 MHz (1.84–2.78 GHz, 40%) for mode 1 and 2, both covering the WLAN band (2.4–2.484 GHz). The measured normalized radiation patterns of the proposed slot antenna for both modes at 2.4 GHz are shown in Figures 4 and 5. Bidirectional radiation is achieved on the Y and $-Y$ axis, and asymmetric patterns are contributed to the effect of the bias structure. For mode 1 shown in Figure 4, the half power beamwidths in the Y–Z plane are 70° (Y direction) and 75° ($-Y$ direction), and while 90° (Y direction) and 90° ($-Y$ direction) in the X–Y plane. For mode 2 in Figure 5, the half power beamwidths in the Y–Z plane are 80° (Y direction) and 70° ($-Y$ direction), and while 110° (Y direction) and 100° ($-Y$ direction) in the X–Y plane. High-level cross-polarization in the radiation patterns is introduced by the parasitic parameters of PIN diodes. Almost the same results as in the Ref. 7 are achieved by using metal strip instead of the PIN diodes in the ON state. Cross polarization can be suppressed by using high-quality PIN diodes with low-parasitic parameters. The measured gain is shown in Figure 6. In the required band, the gain is better than 4.2 and 2.2dBi for mode 1 and 2. The insertion loss of the PIN diodes also decreases the gain performance.

4. MIMO CHANNEL CAPACITY RESULTS

To study the channel capacity improvement of the proposed polarization reconfigurable antenna, a 2 × 2 MIMO system channel measurement was carried out in a typical indoor scenario, shown in Figure 7. Two polarization reconfigurable slot antennas served as transmitter (TX) antennas, representing the AP in the WLAN application. Two dipoles were implemented as the receiver (RX) antennas. To demonstrate the improvement in channel capacity, another two dipoles with single polarization were used as reference TX antennas. The positions of TX and RX antennas are marked in Figure 7. We fixed the TX antennas as AP and moved RX antennas as mobile handset, to simulate the LOS (TX-RX1, TX-RX2) and NLOS (TX-RX3, TX-RX4, TX-RX5) conditions. The space of two antenna elements in TX or RX is 0.5λ, with the mutual coupling less than −25 dB.

TABLE 2 Detailed Dimensions of the Proposed Antenna

Parameter	L	L_S	L_G	L_0	L_1	L_2	L_3	L_4	L_5	W	W_S	W_1	S_1	S_2
Value(mm)	120	50	36	16	8.9	33.9	15.3	20.1	30	80	53	1.9	0.7	1

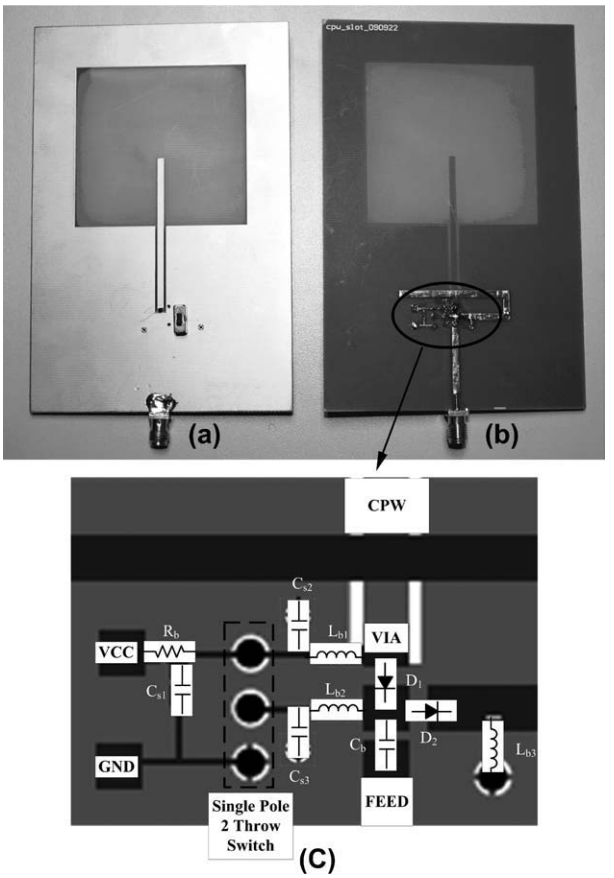

Figure 2 Fabrication of proposed antenna with bias circuit: (a) front side, (b) back side, and (c) bias circuit

The measurement was carried out in the band of 2.2–2.6 GHz, with a step of 2 MHz. Three different orientations (ZZ, YY, and XX) of RX antennas were measured to simulate different operational poses of the mobile handsets. For two horizontal (H) and vertical (V) polarizations reconfigurable antennas, four configurations (HH, HV, VH, VV) were switched manually for each channel capacity measurement in a quasi-static environment, and the best result was chosen for statistics. Given the small-scale fading effect, 4×4 grid locations for each RX position were measured. Therefore, a total $201 \times 3 \times 16 \times 2 = 19{,}296$ measured channel capacity for LOS condition was obtained for statistics, and $201 \times 3 \times 16 \times 3 = 28{,}944$ were the measured results for NLOS condition.

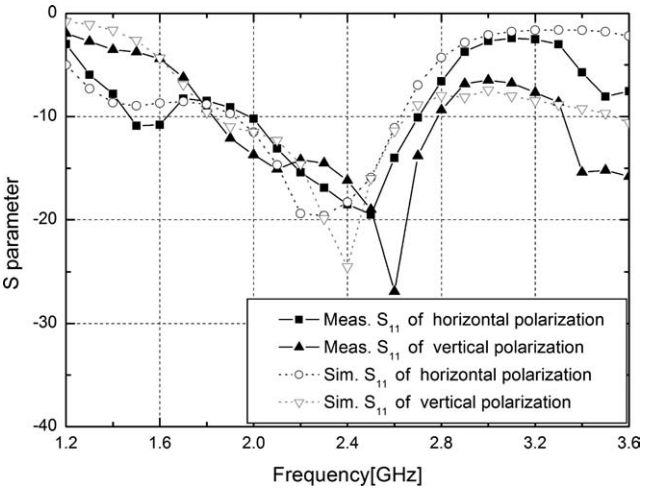

Figure 3 Measured and simulated reflection coefficient

A 4-port vector network analyzer was used to measure the channel response, obtaining a 2×2 MIMO channel matrix $\mathbf{H}$. The channel capacity can be calculated through following formula:

$$C = \log_2 \det[I_{N_r} + \frac{SNR}{N_t} H_n H_n^H] \quad (1)$$

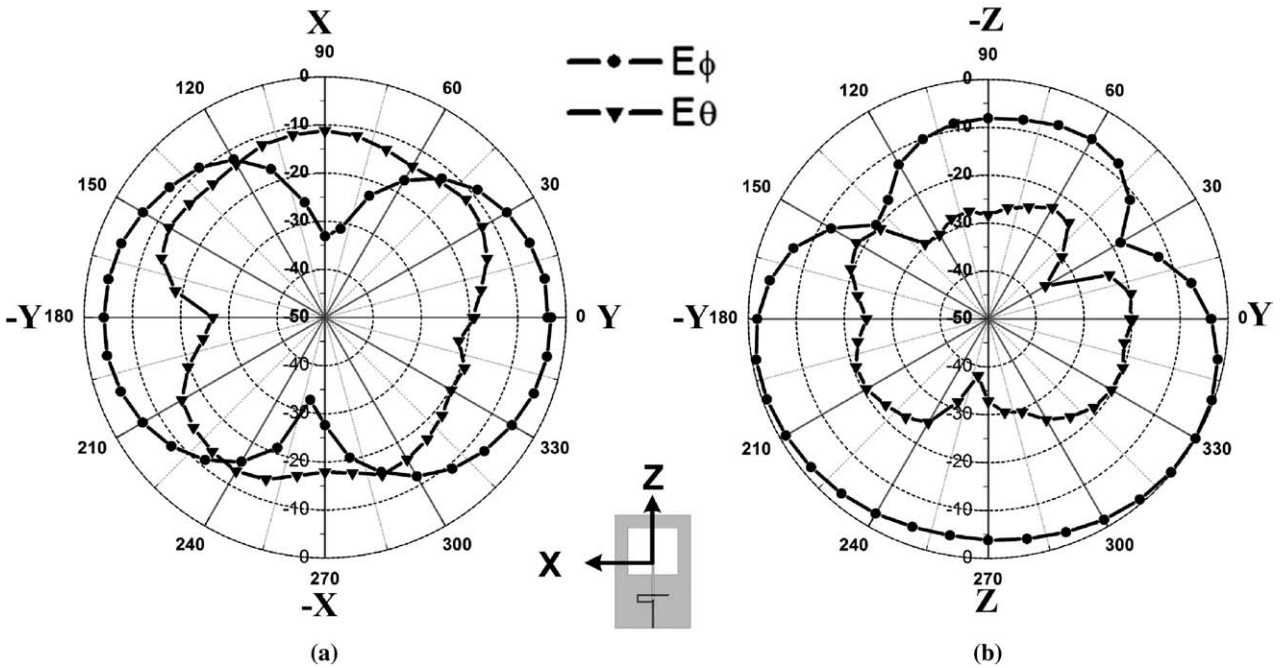

Figure 4 Measured radiation pattern for horizontal polarization at 2.4 GHz. (a) *X–Y* plane and (b) *Y–Z* plane

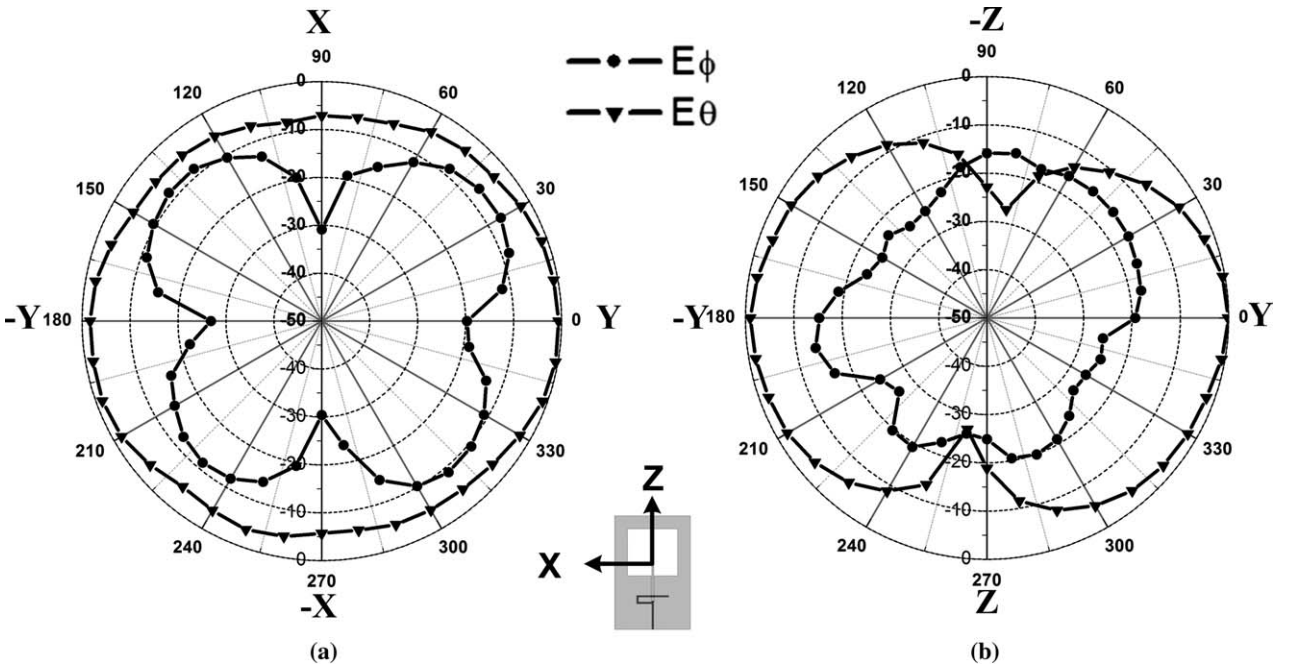

Figure 5 Measured radiation pattern for vertical polarization at 2.4 GHz. (a) *X–Y* plane and (b) *Y–Z* plane

where N_r and N_t are the numbers of RX and TX antennas. $\mathbf{I_{Nr}}$ is a $N_r \times N_r$ identity matrix, SNR is the signal-to-noise ratio at RX position, $\mathbf{H_n}$ is the normalized $\mathbf{H}$, and $()^H$ figures in the Hermitian transpose. $\mathbf{H}$ is normalized by the received power in the 1×1 reference dipole of identical polarization.

The measured channel capacity CCDFs of the proposed polarization reconfigurable antenna in a 2×2 MIMO system in LOS and NLOS conditions are illustrated in Figures 8 and 9, comparing with reference dipoles in 2×2 and 1×1 systems. The SNR used in (1) is determined at an average channel capacity of 5 bit/s/Hz in a 1×1 dipole system in LOS or NLOS. As listed in Table 3, the average and 95% outage capacities are both improved by using polarization reconfiguration, especially in a NLOS situation. For a NLOS indoor scenario, the received energy is mainly contributed from reflection and diffraction, which can vary the polarization of the wave. However, the path loss of NLOS is higher than that of LOS, and the transmitting power should be enhanced to guarantee system performance. Considering the parasitic parameters and insertion loss introduced from nonideal PIN diodes, even better capacity can be achieved by using high quality switches.

5. CONCLUSIONS

A polarization reconfigurable slot antenna with compact feed is proposed and tested. Dual orthogonal polarizations are excited by orthogonal modes of single CPW. Two PIN diodes are

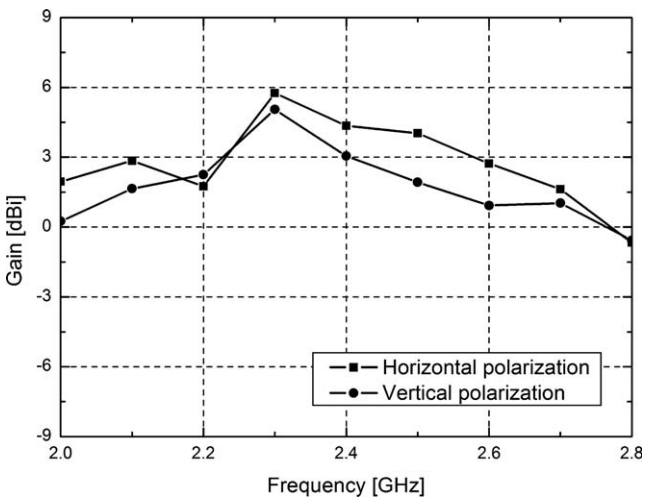

Figure 6 Measured gain

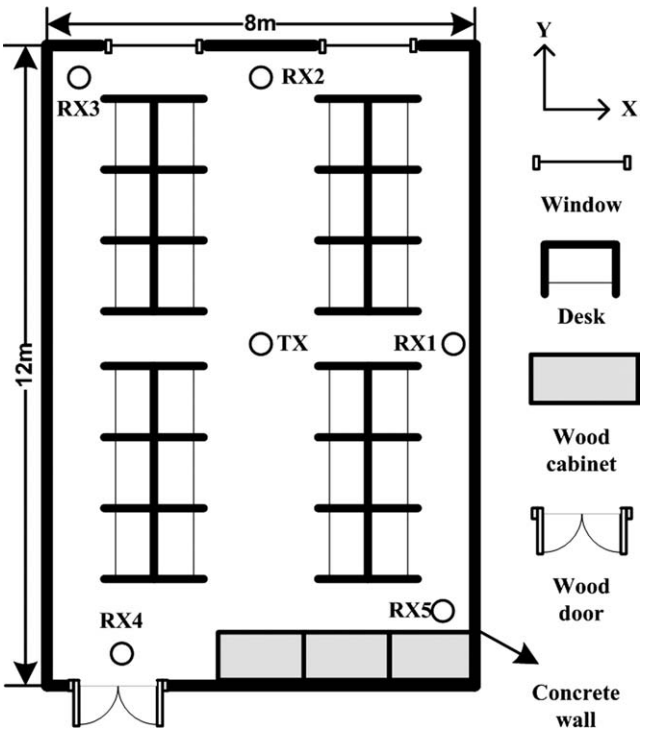

Figure 7 Layout of measurement environment

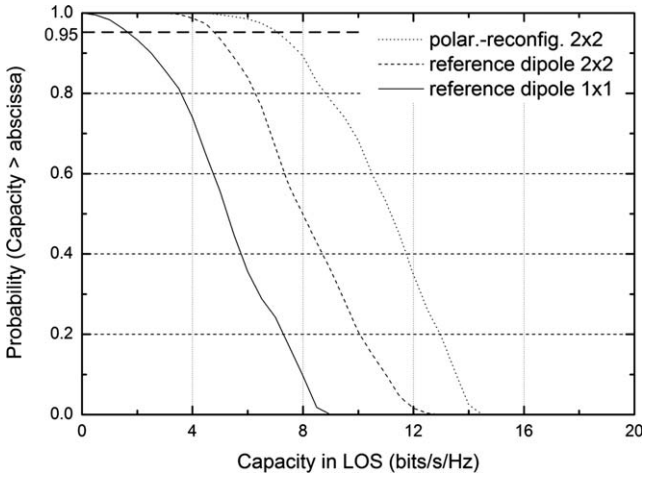

Figure 8 CCDFs of channel capacity in LOS condition

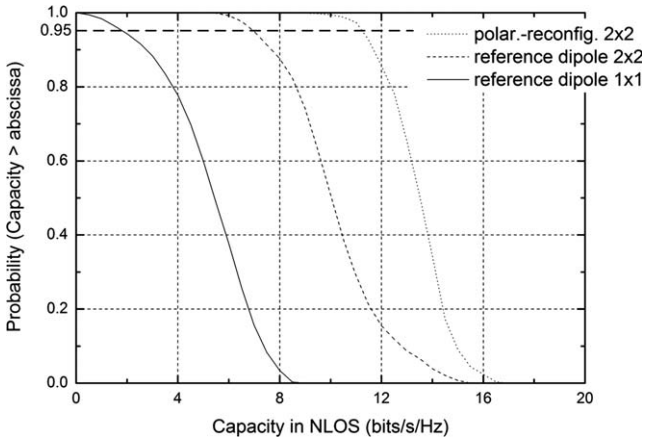

Figure 9 CCDFs of channel capacity in NLOS condition

TABLE 3 Average and 95% Outage Channel Capacity (bit/s/Hz)

Channel capacity	Condition	1 × 1 dipole	2 × 2 dipole	2 × 2 Polar.-reconfig.
Average	LOS	5	7.86	10.62
	NLOS	5	9.9	13.18
95% outage	LOS	1.75	4.91	7.11
	NLOS	1.94	6.87	11.32

adopted to switch the polarizations depending on the propagation condition. The −10 dB reflection coefficients of horizontal and vertical polarizations are 700 MHz (29.2%) and 940 MHz (40%), both covering the WLAN band. The measured gains in required band are better than 4.2 and 2.2 dBi. The channel capacity of the proposed antenna in a 2 × 2 indoor MIMO system has been measured and discussed showing the possible advantage of polarization reconfigurable antennas.

ACKNOWLEDGMENTS

This work is supported by the National Basic Research Program of China under Contract 2009CB320205, in part by the National High Technology Research and Development Program of China (863 Program) under Contract 2007AA01Z284, in part by the National Natural Science Foundation of China under Contract 60771009, and is also supported by the National Science and Technology Major Project of the Ministry of Science and Technology of China 2010ZX03007-001-01.

REFERENCES

1. J.-M. Molina-García-Pardo, J.-V. Rodríguez, and L. Juan-Llácer, Polarized indoor MIMO channel measurements at 2.45 GHz, IEEE Trans Antennas Propag 56 (2008), 3818–3828.
2. J. Sarrazin, Y. Mahé, S. Avrillon, and S. Toutain, collocated microstrip antennas for MIMO systems with a low mutual coupling using mode confinement, IEEE Trans Antennas Propag 58 (2010), 589–592.
3. V. Erceg, H. Sampath, and S. Catreux-Erceg, Dual-polarization versus single-polarization MIMO channel measurement results and modeling, IEEE Trans Wireless Commun 5 (2006), 28–33.
4. Y.B. Chen, Y.C. Jiao, and F.S. Zhang, Polarization reconfigurable CPW-fed square slot antenna using pin diodes, Microwave Opt Technol Lett 49 (2007), 1233–1236.
5. R.-H. Chen and J.-S. Row, Single-fed microstrip patch antenna with switchable polarization, IEEE Trans Antennas Propag 56 (2008), 922–926.
6. S.-H. Hsu and K. Chang, A novel reconfigurable microstrip antenna with switchable circular polarization, IEEE Antennas Wireless Propag Lett 6 (2007), 160–162.
7. Y. Li, Z. Zhang, W. Chen, Z. Feng, and M. F. Iskander, A dual-polarization slot antenna using a compact CPW feeding structure, IEEE Antennas Wireless Propag Lett 9 (2010), 191–194.

A DUAL-BAND GYSEL POWER DIVIDER WITH THE EVEN-MODE INPUT EXTENSION/STUB LINES

Myun-Joo Park and Byungje Lee
Department of Wireless Communications Engineering, Kwangwoon University, 447-1 Wolgye-dong, Nowon-ku, Seoul 139-701, Korea; Corresponding author: mjpark@kw.ac.kr

Received 2 September 2010

ABSTRACT: *A new dual-band structure is proposed for the Gysel power divider. The proposed divider features an extension line at the input and a stub line at the opposite end, both located along the symmetry plane and operating at the even-mode excitation of the divider. The divider is analyzed rigorously to derive the exact design equations in closed-form formula. The design, simulation and experiments based on the proposed method confirm the dual-band capability of the divider.* © 2011 Wiley Periodicals, Inc. Microwave Opt Technol Lett 53:1213–1216, 2011; View this article online at wileyonlinelibrary.com. DOI 10.1002/mop.25979

Key words: *power divider; Gysel power divider; dual-band*

1. INTRODUCTION

Power dividers/combiners are widely used in various wireless circuits and systems to divide or merge the high frequency signals [1]. Among various power dividers developed so far, Wilkinson power dividers are commonly used for the in-phase power division with matched ports and isolated outputs [2]. Gysel power dividers perform similar functions as the Wilkinson power divider and are better suited for high power applications [3–5].

Recently, there have been extensive works concerning the dual-band operation of the power divider [6]. However, most of